Polymer Chemistry

Facile Synthesis of Epoxide-co-Propylene Sulphide Polymers with Compositional and Architectural Control

Journal:	*Polymer Chemistry*
Manuscript ID	PY-ART-01-2022-000005.R1
Article Type:	Paper
Date Submitted by the Author:	14-Mar-2022
Complete List of Authors:	Safaie, Niloofar; Michigan State University, Chemistry Smak, Jessica; Michigan State University, Chemical Engineering and Materials Science DeJonge, Danielle; Michigan State University, Chemical Engineering and Materials Science Cheng, Shiwang; Michigan State University, Chemical Engineering and Materials Science Zuo, Xiaobing; Argonne National Laboratory, Ohno, Kohji; Institute for Chemical Research, Kyoto University, Ferrier, Jr., Robert; Michigan State University, Chemical Engineering and Materials Science

ARTICLE

Facile Synthesis of Epoxide-co-Propylene Sulphide Polymers with Compositional and Architectural Control

Niloofar Safaie[a], Jessica Smak[b], Danielle DeJonge[b], Shiwang Cheng[b], Xiaobing Zuo[c], Kohji Ohno*[d], Robert C. Ferrier, Jr.*[b]

Received 00th January 20xx,
Accepted 00th January 20xx

DOI: 10.1039/x0xx00000x

We present a facile method to produce propylene sulphide (PS) homopolymers up to 100 kg/mol and PS – epoxide statistical, block, and ABA copolymers using inexpensive and versatile thio-aluminium (SAl) based initiators. Homopolymerizations of PS with SAl initiators are living and controlled, with number averaged molecular weights ($\overline{M}_n$) up to 100 kg/mol while maintaining narrow polydispersity (Đ < 1.4). Statistical and block copolymers of PS and epichlorohydrin (ECH) or propylene oxide (PO) are synthesized and characterized by size-exclusion chromatography (SEC), differential scanning calorimetry (DSC), ^{1}H and ^{13}C NMR spectroscopy, diffusion ordered spectroscopy (DOSY), and small-angle X-ray scattering (SAXS). This work represents the first statistical copolymerization of PS and epoxides with similar reactivity ratios, allowing fine control over composition. Block-copolymers of PS and epoxides are synthesized by sequential addition, without intermediate preparative steps. Polymer architecture is controlled through modification of the initiator; we synthesized a di-functional (d-H) SAl initiator to produce ABA tri-block-copolymers. Finally, poly(ethylene glycol) (PEG) was used as a macroinitiator to create PEG-*b*-PPS block copolymers and characterized by ^{1}H, ^{13}C NMR spectroscopy, DOSY, DSC, and SEC.

Introduction

Poly(propylene sulphide) (PPS) is a versatile, non-toxic, sulphur-containing polymer that has widespread use in biomedical[1-3] and patterning[4, 5] contexts. The sulphur in the polymer backbone can readily be converted to hydrophilic sulfone groups in the presence of oxidative species, making PPS ideal for targeted drug delivery.[6] Additionally, PPS consisting of pure converted sulfone groups undergoes interesting solvent-mediated self-assembly.[7] Sigwalt and co-workers demonstrated classical anionic polymerization of PS in the 1960's using sodium naphthalene as an initiator.[8] Modern anionic synthesis of PPS utilizes thiolate anions as an initiator either produced directly from deprotonation of a thiol or via protected thiol ala acyl group transfer.[6] While these methods are effective, they typically produce polymers with molecular weight *ca.* 10 kg/mol. Very recent work by Rumyantsev demonstrated PPS at molecular weights above 100 kg/mol at Đ < 1.4 using xanthates, but molecular weight control was not straightforward.[9] Initiation from thiolates is robust, and several thiols with a variety of chemistries and structures are available for end group and / or architecture control. For instance, dithiols can be employed to create ABA co-polymers[10] and multi-armed thiols[11, 12] can be used to create star polymers. This architectural and chemical control over PPS, along with the ability of PPS to switch from a hydrophobic to hydrophilic character as well as PPS inherent biocompatibility has made it practically ubiquitous as a component in drug delivery schemes.

PPS is frequently paired with other biologically relevant polymers. PPS acts as the hydrophobic block in a block copolymer paired with a hydrophilic polymer, like poly(ethylene glycol) (PEG). Amphiphilic block copolymers consisting of PPS and another hydrophilic block have been used to create vesicular[13, 14] and micellar structures[11] through self-assembly that hold medicinal cargo, which can be released in the presence of oxidative species that causes the PPS block to become hydrophilic. Hubbell and Tirelli have developed synthetic methods for block-co-polymers containing PPS. Typically, either a macroinitiator[6, 15, 16] or a coupling strategy[16] is employed for block copolymer synthesis; in the former case the second polymer is polymerized from the first polymer and in the latter case two pre-formed polymers are coupled end to end (*e.g.*, through a 'click' reaction). Both methods require multiple steps. Recently, Frey and co-workers[17] demonstrated the use of a multifunctional initiator, cysteine, to synthesize copolymers of PPS and sarcosine of varying ratio by a protection / de-protection strategy for the cysteine. Wang and co-workers employed a combined RAFT and AROP polymerization strategy to copolymerize PPS with N-isopropylmethacrylamide (NIPMAM).[18] However, this resulted in some incorporation of the NIPMAM into the PS block. Developing facile synthetic

[a] *Department of Chemistry, Michigan State University, East Lansing, Michigan 48824, United States.*
[b] *Department of Chemical Engineering and Materials Science, Michigan State University, East Lansing, Michigan 48824, United States. Email: ferrier5@egr.msu.edu*
[c] *X-ray Science Division, Argonne National Laboratory, Lemont, Illinois, 604393.*
[d] *Institute for Chemical Research, Kyoto University, Kyoto 611-0011, Japan. Email: ohno@scl.kyoto-u.ac.jp*

† Electronic Supplementary Information (ESI) available: ^{1}H and ^{13}C NMR spectra for initiators and polymers. DOSY spectra for copolymers. SAXS data. Kinetic plots for polymerizations. SEC traces for polymers. DSC curves for polymers. Experimental methods. See DOI: 10.1039/x0xx00000x-

techniques that allow for synthesizing PS containing block copolymers, especially those with epoxides, through sequential addition of monomer would allow for finer control over copolymer physical properties and increase access to these materials.

Aside from block copolymers, copolymers containing both ethers and sulphur in the backbone have found use in optical and electronic applications.[19, 20] Frequently, these polymers are produced through the alternating copolymerization of epoxides and sulphur containing species like carbonyl sulphide[21] and carbon disulphide.[22] Aside from alternating copolymers, limited compositional control over copolymers from epoxides and thiol containing monomers has been demonstrated. Episulphides in particular are difficult to copolymerize with epoxides due to the propensity of the episulphide to homopolymerize[20, 23] resulting in block- instead of statistical-copolymers. While some patents exist involving statistical-copolymers of epoxides and episulphides, they only achieve a small percentage (<10%) of epoxide incorporation.[24, 25] Diversifying the epoxide monomers compatible with PS in copolymerization schemes will allow for new PPS materials with tuneable or unique property sets.

In this work, we investigate our previously reported thio-aluminium (SAl) initiators[26] with alkyl amine-aluminium (NAl) catalyst for PS and PS-co-epoxide polymerizations. We explore molecular weight control of PPS by tuning PS to initiator ratio and quantify this by size exclusion chromatography (SEC) and NMR spectroscopy. The influence of catalyst and initiator interaction on polymerization control and kinetics is characterized through ^{1}H NMR spectroscopy and SEC. Copolymerization of PS and epoxides are performed to determine polymer compositional control. Finally, we demonstrate both block and statistical copolymers and characterize these polymers through ^{1}H, ^{13}C, and diffusion ordered NMR spectroscopy as well as SEC, differential scanning calorimetry (DSC), and small angle X-ray scattering (SAXS). Initiator chemistry was varied to control polymer architecture, and we synthesized ABA (co)polymers. Synthesis of biomedically applicable poly(EG-*b*-PS) was achieved by the addition of PS to macroinitiator PEG. This work demonstrates methods that allow for the direct synthesis of PS-block-epoxide polymers as well as the statistical copolymerization of PS and epoxide, which has been difficult to achieve in the past.

Materials and Methods

Materials

Trimethylaluminium solution (AlMe3, 2.0 M in hexane), triethylamine (TEA, ≥99.5%), benzyl mercaptan (99%), benzyl alcohol, 1-propane thiol (99%), 1,3-propanedithiol (Sigma-Aldrich, 99%), pentaerythritol tetrakis(3-mercaptopropionate) (99%), and poly(ethylene glycol) (5500 g/mol) were purchased from Sigma-Aldrich. CDCl3 (Cambridge Analytica) was used without any further purification. Hexanes (Sigma Aldrich, anhydrous, >99%) was used for initiator / catalyst purification in the glovebox. Methanol (MeOH, Fisher, Certified ACS), hexane (Fisher, Certified ACS), and dichloromethane (DCM, Fisher, Certified ACS) were used for washing the polymers. Propylene sulphide (PS, 96%, ACROS Organics), propylene oxide (PO, Sigma-Aldrich, GC, ≥99.5%), and epichlorohydrin (ECH, Sigma-Aldrich, ≥99%), were all used as received. All air and moisture-sensitive reactions were prepared under a dry nitrogen atmosphere inside a glovebox.

Characterization

^{1}H NMR spectroscopy was performed on a 500 MHz Varian NMR spectrometer at room temperature, and chemical shifts are reported in parts per million (ppm), referenced using the residual ^{1}H peak from the deuterated solvent. The structure of the compounds was determined by ^{13}C NMR spectroscopy on a 126 MHz Varian NMR spectrometer. All diffusion ordered spectroscopy (DOSY) measurements were performed at 25 °C on a Varian Inova 600 spectrometer operating at 599.72 MHz and equipped with a 5 mm Z-gradient HCN inverse probe capable of producing gradients in the Z direction with a strength of 63 G/cm. All DOSY measurements were run using the dbppste pulse sequence with 128−160 scans and 20 increments with gradient strengths from 2.7 to 59.22 G/cm. The relaxation delay was set to 3 s, the diffusion delay to 24 ms, and the gradient length to 2.0 ms. Size-exclusion chromatography (SEC) was carried out on the Malvern OMNISEC system with an isocratic pump, degasser, and temperature-controlled column oven held at 35 °C containing 2 Viscotek 300 × 8.0 mm^2 columns (T3000 and T4000) with an exclusion limit of 400 kDa. Triple detection with light scattering, viscometer, and the refractive index has been used for the absolute molecular weight determination of the polymers. The reported $\overline{M}_n$ are all absolute molecular weights. Differential scanning calorimetric (DSC) tests were conducted on a TA250 instrument with a heating rate of 10 °C/min under a N_2 atmosphere, and the data from the second heating curve were collected. PPS homopolymer was analysed by electrospray ionization with mass spectrometry (ESI-MS) in positive ion mode using a Waters Xevo G2XS Q-Tof mass spectrometer interfaced with a Waters Acquity UPLC. Five µL of a sample (diluted in 90% methanol containing 1 mM ammonium formate) was flow-injected (no UPLC column) using a mobile phase of 80% methanol and 20% 10 mM ammonium formate in water pumped at 0.2 mL/min. SAXS measurements were performed at the beamline 12-ID-B at Advanced Photon Source of Argonne National Laboratory with the x-ray energy of 13.3 keV with a two-dimensional (2-D) Pilatus 2M detector. The sample to detector distance was set to 2.0 m. In all measurements, the sample thickness was kept around 0.1 mm and the exposure time of 0.5 s. The scattering of the air has been measured as the background noise. The scattering intensity is obtained from converting the 2-D spectra into 1-D, using the beamline software.

Synthesis of trimethylaluminium and triethylamine (NAl) adduct catalyst

In a reaction vial with a stir bar, 6.35 mL of anhydrous hexanes and 2.0 M $AlMe_3$ in hexane (6.35 mL, 12.7 mmol) were added and cooled to −78 °C. Then, triethylamine (1.5 mL, 10.7 mmol)

was added dropwise into the vial. The solution was set to stir and warm to room temperature overnight. To crystallize the desired product, the solution was then directly cooled to −40 °C and the resultant crystals were washed three times with anhydrous hexanes (3 × 5 mL) and dried in *vacuo*. ^{1}H NMR (500 MHz, $CDCl_3$) δ 2.80 (q, 6H, $_3(CH_3C\underline{H}_2)N{:}Al(CH_3)_3$), 1.18 (t, 9H, $_3(C\underline{H}_3CH_2)N{:}Al(CH_3)_3$), −0.89 (s, 9H, $_3(CH_3CH_2)N{:}Al(C\underline{H}_3)_3$). ^{13}C NMR (126 MHz, $CDCl_3$) δ 64.54 $_3(CH_3\underline{C}H_2)N{:}Al(CH_3)_3$), 47.78 $_3(\underline{C}H_3CH_2)N{:}Al(CH_3)_3$, 9.20 $_3(CH_3CH_2)N{:}Al(\underline{C}H_3)_3$).

General Procedure for Synthesis of Initiators

In a 20 mL vial or a 100 mL round-bottom reaction flask, anhydrous hexane (6.35 mL) and 2.0 M $AlMe_3$ in hexanes (6.35 mL, 12.7 mmol) were added and cooled down to −78 °C. Then, mono-functional (benzyl mercaptan/benzyl alcohol/propyl thiol), di-functional (propane dithiol), or tetra-functional (pentaerythritol tetrakis (3- mercaptopropionate)) (12.7 mmol) was added dropwise, and the solution was stirred for 24 h while warming to room temperature. To remove unreacted $AlMe_3$ and purify the initiator, the synthesized compound was washed three times with anhydrous hexanes and dried *in vacuo*. Volumes of hexane and $AlMe_3$ were doubled or quadrupled for di-functional or tetrafunctional ligands.

Benzyl Mercaptan – Dimethyl Aluminium ($BnSAlMe_2$)

^{1}H NMR and ^{13}C NMR spectrum of $BnSAlMe_2$. ^{1}H NMR (500 MHz, $CDCl_3$) δ 7.38 to 7.21 (m, 5H, $\underline{Ph}CH_2S\text{-}Al(CH_3)_2$), 3.91 (s, 2H, $PhC\underline{H}_2S\text{-}Al(CH_3)_2$), -0.43 (s, 6H, $PhCH_2SAl(C\underline{H}_3)_2$). ^{13}C NMR (126 MHz, $CDCl_3$) δ141.46, 128.56, 127.97, 126.89 ($\underline{Ph}CH_2S\text{-}Al(CH_3)_2$, 32.00 ($Ph\underline{C}H_2S\text{-}Al(CH_3)_2$), 28.78 ($PhCH_2S\text{-}Al(\underline{C}H_3)_2$).

Benzyl Alcohol – Dimethyl Aluminium ($BnOAlMe_2$)

^{1}H NMR (500 MHz, $CDCl_3$) δ 7.47 – 7.38 (m, 5H, $\underline{Ph}CH_2O\text{-}Al(CH_3)_2$), 3.33 (s, 2H, $PhC\underline{H}_2O\text{-}Al(CH_3)_2$), 0.15 - -0.6 (s, 6H, $PhCH_2OAl(C\underline{H}_3)_2$). b) ^{13}C NMR (126 MHz, $CDCl_3$) δ138.64, 137.57, 130.04, 126.69 ($\underline{Ph}CH_2O\text{-}Al(CH_3)_2$, 50.76 ($Ph\underline{C}H_2O\text{-}Al(CH_3)_2$), -7.71 ($PhCH_2O\text{-}Al(\underline{C}H_3)_2$).

Propyl Thiol – Dimethyl Aluminium ($PrSAlMe_2$)

^{1}H NMR (500 MHz, $CDCl_3$) δ 2.62 (m, 2H, $CH_3CH_2C\underline{H}_2S\text{-}Al(CH_3)_2$), 1.65 (dq, 2H, $CH_3C\underline{H}_2CH_2S\text{-}Al(CH_3)_2$), 1.04-0.95 (m, 3H, $C\underline{H}_3CH_2CH_2S\text{-}Al(CH_3)_2$), -0.49 (S, 6H, $CH_3CH_2CH_2S\text{-}Al(C\underline{H}_3)_2$). ^{13}C NMR (126 MHz, $CDCl_3$) δ 30.33 ($CH_3CH_2\underline{C}H_2S\text{-}Al(CH_3)_2$), 25.97 ($CH_3\underline{C}H_2CH_2S\text{-}Al(CH_3)_2$), 13.15 ($\underline{C}H_3CH_2CH_2S\text{-}Al(CH_3)_2$), -9.21 ($CH_3CH_2CH_2S\text{-}Al(\underline{C}H_3)_2$).

1,3 Propane Dithiol – Dimethyl Aluminium (d-H)

^{1}H NMR and ^{13}C NMR spectra of the d-H initiator. ^{1}H NMR (500 MHz, $CDCl_3$) δ 3.41-1.70 (b, $_2(CH_3)Al\text{-}C\underline{H}_2C\underline{H}_2C\underline{H}_2S\text{-}Al(CH_3)_2$, 6H). -0.24 to -0.92 (b, $_2(C\underline{H}_3)Al\text{-}CH_2CH_2CH_2S\text{-}Al(C\underline{H}_3)_2$, 6H), ^{13}C NMR (126 MHz, $CDCl_3$) δ 29.65 $_2(CH_3)Al\text{-}\underline{C}H_2CH_2\underline{C}H_2S\text{-}Al(CH_3)_2$, 27.73 $_2(CH_3)Al\text{-}CH_2\underline{C}H_2CH_2S\text{-}Al(CH_3)_2$, 11.31 $_2(\underline{C}H_3)Al\text{-}CH_2CH_2CH_2S\text{-}Al(\underline{C}H_3)_2$.

General Procedure for Synthesis of Polymers

All polymerizations were performed neat in a septum-capped reaction vial unless otherwise noted. The vials were charged with a stir bar, monomer(s), NAl, and initiator under inert environment. For example, to target 30 kg/mol poly(propylene sulphide) initiated with $BnSAlMe_2$: $BnSAlMe_2$ (0.018 g, 0.01 mmol), NAl (0.0175 g, 0.01 mmol), and propylene sulphide (3.19 mL, 3g, 0.040 mol). The initiator to monomer ratio controls molecular weight. Catalyst concentration is pinned at the values above regardless of molecular weight. This was chosen as it provides a good mix of fast kinetics and control. Please see the cited works for further details on catalyst activity.[27, 28] Block-co-polymers were synthesized via sequential addition of monomers. Solution were heated to 50 °C until the completion of the polymerization. The reaction was quenched with methanol and dissolved in dichloromethane. The resulting solution was added dropwise into acidic MeOH (0.01 M HCl in MeOH) to precipitate and washed three times with water to remove residual aluminium. After precipitation out of MeOH, the polymer was dried *in vacuo* overnight at 70 °C. SEC with refractive index, light scattering, and viscosity detectors determined absolute molecular weights and Đ. $\overline{M}_n$ was determined by ^{1}H NMR spectroscopy by taking the ratio of the backbone proton signals to the integral of the end group signal on the initiator. Resultant polymers were characterized by ^{1}H NMR spectroscopy, ^{13}C NMR spectroscopy, and DSC. Block and statistical copolymers were further characterized by DOSY NMR spectroscopy.

Poly(propylene sulphide) (PPS)

^{1}H NMR (500 MHz, $CDCl_3$) δ 2.91-2.80 (m, −S−CH_2−C$\underline{H}$(CH_3)−S−), 2.65-2.58 (m, −S−C$\underline{H}_2$−CH(CH_3)−S−), 1.39 (m, −S−CH_2−CH(C$\underline{H}_3$)−S−). ^{13}C NMR (126 MHz, $CDCl_3$) δ 41.14 (−S−CH_2−$\underline{C}$H(CH_3)−S), 38.18 (−S−$\underline{C}H_2$−CH(CH_3)−S), 20.63 (−S−CH_2−CH($\underline{C}H_3$)−S−).

Poly[(epichlorohydrin)-co-(propylene sulphide)] (Poly(ECH-*stat*-PS))

^{1}H NMR (500 MHz, $CDCl_3$) δ 3.80-3.29 (bm, −O−C$\underline{H}_2$−C$\underline{H}$($C\underline{H}_2$Cl)−O−), 3.16-2.51 (bm, −S−C$\underline{H}_2$−C$\underline{H}$(CH_3)−S−), 1.63-1.54 (m, −O−CH_2−C$\underline{H}$(CH_2Cl)−O− and −S−CH_2−C$\underline{H}$(CH_3)−S−), 1.40-1.33 (m, −S−CH_2−CH(C$\underline{H}_3$)−S−), 1.37-1.17 O−C$\underline{H}_2$−CH(CH_2Cl)−O− and −S−C$\underline{H}_2$−CH(CH_3)−S−). ^{13}C NMR (126 MHz, $CDCl_3$) 79.37(−O−CH_2−$\underline{C}$H(CH_2Cl)−O−), 75.58 (−O−$\underline{C}H_2$−CH(CH_2Cl)−O−), 44.72 (−O−CH_2−CH($\underline{C}H_2$Cl)−O−), 41.16 (−S−CH_2−$\underline{C}$H(CH_3)−S−), 38.39 (−O−CH_2−$\underline{C}$H(CH_2Cl)−O− and −S−CH_2−$\underline{C}$H(CH_3)−S−), 20.63 (−S−$\underline{C}H_2$−CH(CH_3)−S−), 20.85 (−O−$\underline{C}H_2$−CH(CH_2Cl)−O− and −S−$\underline{C}H_2$−CH(CH_3)−S−), 18.59 (−S−CH_2−CH($\underline{C}H_3$)−S−).

Poly[(propylene oxide)-co-(propylene sulphide)] (Poly(PO-*stat*-PS))

^{1}H NMR (500 MHz, $CDCl_3$) δ 3.83-3.24 (bm, −O−C$\underline{H}_2$−C$\underline{H}$(CH_3)−O−), 3.10-2.41 (bm, −S−C$\underline{H}_2$−C$\underline{H}$(CH_3)−S−, −O−CH_2−C$\underline{H}$(CH_3)−O− and −S−CH_2−C$\underline{H}$(CH_3)−S−), 1.32-1.42 (m, −S−CH_2−CH(C$\underline{H}_3$)−S−), 1.30-1.19 (bm, −O−C$\underline{H}_2$−CH(CH_3)−O− and −S−C$\underline{H}_2$−CH(CH_3)−S−), 1.17-1.04 (m, −O−CH_2−CH(C$\underline{H}_3$)−O−).^{13}C NMR (126 MHz, $CDCl_3$) δ75.85 (−O−CH_2−$\underline{C}$H(CH_3)−O−), 73.34 (−O−$\underline{C}H_2$−CH(CH_3)−O−), 72.90 (−O−CH_2−$\underline{C}$H(CH_3)−O− and −S−CH_2−$\underline{C}$H(CH_3)−S), 41.23 (−S−CH_2−$\underline{C}$H(CH_3)−S−), 38.10 (−S−$\underline{C}H_2$−CH(CH_3)−S−), 20.8 (−O−$\underline{C}H_2$−CH(CH_3)−O− and

–S–$\underline{C}H_2$–CH(CH_3)–S), 19.3 (–S–CH_2–CH($\underline{C}H_3$)–S–), 17.4 (–O–CH_2–CH($\underline{C}H_3$)–O–)

Poly([epichlorohydrin]-co-[propylene sulphide]) (Poly(ECH-*b*-PS))

^{1}H NMR (500 MHz, $CDCl_3$) δ 3.72–3.2 (bm, –O–$C\underline{H}_2$–$C\underline{H}$(CH_3)–O–), 2.91-2.54 (bm, –S–$C\underline{H}_2$–$C\underline{H}$(CH_3)–S–), 1.31 (m, –S–CH_2–CH($C\underline{H}_3$)–S–), 1.11 (m, –O–CH_2–CH($C\underline{H}_3$)–O–). ^{13}C NMR (126 MHz, $CDCl_3$) δ 78.97 (–O–CH_2–$\underline{C}H$(CH_2Cl)–O–), 69.51 (–O–$\underline{C}H_2$–CH(CH_2Cl)–O), 43.47 (–O–CH_2–CH($\underline{C}H_2Cl$)–O–), 41.17 (–S–CH_2–$\underline{C}H$(CH_3)–S–), 38.24 (–S–$\underline{C}H_2$–CH(CH_3)–S–), 20.86 (–S–CH_2–CH($\underline{C}H_3$)–S–).

Poly([propylene oxide]-co-[propylene sulphide]) (Poly(PO-*b*-PS))

^{1}H NMR (500 MHz, $CDCl_3$) δ 3.77-3.55 (bm, –O–$C\underline{H}_2$–$C\underline{H}$($C\underline{H}_2Cl$)–O–), 2.91-2.80 (m, –S–$C\underline{H}_2$–CH(CH_3)–S–), 2.65-2.58 (m, –S–CH_2–$C\underline{H}$(CH_3)–S–), 1.35 (m, –S–CH_2–CH($C\underline{H}_3$)–S–). ^{13}C NMR (126 MHz, $CDCl_3$) δ 75.26 (–O–CH_2–$\underline{C}H$(CH_3)–O–), 73.35 (–O–$\underline{C}H_2$–CH(CH_3)–O–), 40.6 (–S–CH_2–$\underline{C}H$(CH_3)–S–), 37.9 (–S–$\underline{C}H_2$–CH(CH_3)–S–), 20.98 (–S–CH_2–CH($\underline{C}H_3$)–S–), 16.83 (–O–CH_2–CH($\underline{C}H_3$)–O–).

Poly(PO-*b*-PS) Initiated with d-H

^{1}H NMR (500 MHz, $CDCl_3$) δ 3.72–3.2 (bm, –O–$C\underline{H}_2$–$C\underline{H}$(CH_3)–O–), 2.91-2.54 (bm, –S–$C\underline{H}_2$–$C\underline{H}$(CH_3)–S–), 1.31 (m, –S–CH_2–CH($C\underline{H}_3$)–S–), 1.11 (m, –O–CH_2–CH($C\underline{H}_3$)–O–). ^{13}C NMR (126 MHz, $CDCl_3$) δ 75.26 (–O–CH_2–$\underline{C}H$(CH_3)–O–), 73.35 (–O–$\underline{C}H_2$–CH(CH_3)–O–), 40.6 (–S–CH_2–$\underline{C}H$(CH_3)–S–), 37.9 (–S–$\underline{C}H_2$–CH(CH_3)–S–), 20.98 (–S–CH_2–CH($\underline{C}H_3$)–S–), 16.83 (–O–CH_2–CH($\underline{C}H_3$)–O–).

Poly([ethylene glycol]-co-[propylene sulphide]) (poly(EG-b-PS))

In a vial equipped with a stir bar, 1.5 g of PEG dissolved in 3 ml anhydrous benzene and purged with N_2. After dissolution, 0.1 ml of $AlMe_3$ solution was added dropwise to the dissolved PEG forming a macroinitiator. Further, PS (1 g, 0.013 mol, 0.092 ml) and NAl (0.03 g, 0.041 mmol) were added to the solution, and the reaction heated up to 50 °C overnight. After full consumption of PS, the solution was exposed to air and, the excess benzene was evaporated. The residue then dissolved in 2 ml DCM, precipitated out of MeOH, and dried on the vacuum at 70 °C. ^{1}H NMR (500 MHz, $CDCl_3$) δ 3.65-3.48 (b, –O–CH_2–CH_2–O–), 2.92-2.78 80 (m, –S–CH_2–CH(CH_3)–S–), 2.66-2.59 (m, –S–CH_2–CH(CH_3)–S–), 1.38 (m, –S–CH_2–CH(CH_3)–S–). ^{13}C NMR (126 MHz, $CDCl_3$) δ 70.55 (–O–CH_2–CH_2–O–), 41.26 (–S–CH_2–CH(CH_3)–S–), 38.38 (–S–CH_2–CH(CH_3)–S–), 20.79 (–S–CH_2–CH(CH_3)–S–).

Kinetics Studies of PS Polymerization with ^{1}H NMR Spectroscopy

Polymerizations were performed as previously described. Aliquots (*ca.* 30 µL) of the reaction were taken every 15 minutes and immediately dissolved in $CDCl_3$ and reactions quenched by exposing to air. Conversion was determined using ^{1}H NMR spectroscopy. The conversion of each monomer was calculated based on the integration of the backbone area to the unreacted corresponding monomer by ^{1}H NMR spectroscopy.

Results and Discussions

Previously, we developed a thio-aluminium based (SAl) initiator that quickly and controllably polymerized epoxides in the presence of a Lewis pair (LP) catalyst consisting of triethyl amine and trimethyl aluminium (NAl).[26] Briefly, we believe the initiator serves to coordinate with the monomer ala a mechanism reminiscent of the Vandenberg catalyst.[27] The catalyst serves to activate the monomer for ring opening ala a mechanism reminiscent of monomer activated ring opening polymerization (MAROP)[29-31]. Further details of the SAl initiatior for epoxide polymerization can be found in the citation.[28] Details of the effect of the catalyst on polymerization kinetics can be found in this citation.[27] Mechanistic insights can be found in a recent PhD thesis by Dr. Imbrogno[32] as well as a forthcoming publication from the Ferrier group. Since we suspect initiation occurs from a thiolate ion, we hypothesized that this would be amenable to episulphide polymerization. To test this idea, we investigated the homopolymerization of propylene sulphide (PS) with our SAl initiator ($BnSAlMe_2$) and NAl (Et_3NAlMe_3) catalyst. $BnSAlMe_2$ and NAl were synthesized by previously reported methods.[26, 27] PS polymerization was performed neat at 50 °C in the presence of $BnSAlMe_2$ and NAl catalyst in an equimolar ratio, which resulted in PPS with a yield of 94.2% after purification procedure. A scheme of this reaction can be seen in **Scheme 1**. PPS was characterized via size-exclusion chromatography (SEC) with triple detection and the absolute $\overline{M}_n$ was found to be 33.7 kg/mol with polydispersity (Đ) = 1.21 (**Figure 1b, purple line**), consistent with the targeted molecular weight of 30 kg/mol. The $\overline{M}_n$ determined by SEC compared favourably to the molecular weight calculated through ^{1}H NMR spectroscopy via end group analysis of 36.2 kg/mol (SI, **Figure S1a**). The ^{13}C NMR revealed an atactic PPS, in line with polyethers synthesized previously.[26] The results for this polymerization can be found in **Table 1**, entry 2. It should be noted that the polymerization time in the table refers to the time at which the polymerization was terminated with conversion > 99%. This polymer was further characterized by differential scanning calorimetry (DSC) and showed one glass transition temperature (T_g) at –41 °C (SI, **Figure S2**), in accordance with the literature value.[33]

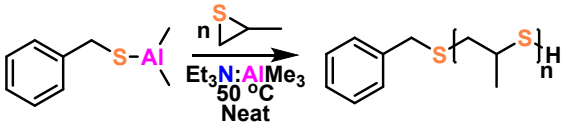

Scheme 1. Scheme for polymerization of propylene sulphide using $BnSAlMe_2$.

Entry	Polymer	Initiator	Time(hr.)[a]	$\overline{M}_{n}$(theo) (kg/mol)	$\overline{M}_{n}$[b](kg/mol)	$\overline{M}_{n}$[c](kg/mol)	Đ[c]

1	PPS	$BnSAlMe_2$	6	15	14.8	14.3	1.20
2	PPS	$BnSAlMe_2$	10	30	33.7	36.2	1.21
3	PPS	$BnSAlMe_2$	48	50	47.1	46.7	1.32
4	PPS	$BnSAlMe_2$	70	70	68.4	67.7	1.35
5	PPS	$BnSAlMe_2$	102	100	98.2	97.1	1.24
6	P(ECH-*stat*-PS)	$BnSAlMe_2$	168	30	29.2	27.3	1.56
7	P(PO-*stat*-PS)	$BnSAlMe_2$	72	30	30.8	28.6	1.21
8	P(ECH-*b*-PS)	$BnSAlMe_2$	168	30	29.9	30.3	1.74
9	P(PO-*b*-PS)	$BnSAlMe_2$	72	30	29.6	27.8	1.32
10	PPS	d-H	5	30	34.5	-	1.37
11	P(PS-*b*-PO)	d-H	24	30	29.8	-	1.39
12	PPS	$PrSAlMe_2$	5	30	32.3	31.1	1.21
13	PPS	$BnOAlMe_2$	48	30	31.7	32.4	1.24
14	P(EG-*b*-PS)[e]	$mPEGAlMe_2$	18	20	22.2	23.8	1.18

Table 1. Summary of (co)polymers synthesized

[a] Time terminated at > 99% conversion as determined by ^{1}H NMR spectroscopy. [b] Absolute molecular weight and Đ determined from SEC with LS, RI, and viscometry triple detection system. [c] Determined from end group analysis of the ^{1}H NMR spectra. [d] Polymerizations were conducted at room temperature. Reaction condition: NAI (1 mmol), initiator (1 mmol), PS (0.4 mol), and for synthesis of copolymers we used (1:1) ratio of monomers. [e] Initiated from macroinitiator.

Control over PPS molecular weight was achieved by varying the monomer to initiator ratio ($[M_0]/[I_0]$) with constant catalyst concentration (63.5 µM). Molecular weights of 15, 30, 50, 75, and 100 kg/mol were targeted. Here, we have direct control over $\overline{M}_n$ through $[M_0]/[I_0]$, which differs from a recent report that demonstrates high $\overline{M}_n$ PPS.[9] The $\overline{M}_n$ determined by SEC and end group analysis via ^{1}H NMR spectroscopy was consistent with the targeted molecular weights. **Figure 1a** is a plot of the molecular weight (left) and Đ (right) as a function of the $[M_0]/[I_0]$. A linear fit (blue line) to the molecular weight data is provided to emphasize the controlled nature of the polymerization. The commensurate SEC traces for these polymers can be seen in **Figure 1b** The molecular weight was narrow with Đ ≈ 1.25 in most cases, further suggesting a controlled polymerization. We also synthesized 5 kg/mol PPS and characterized it with ESI-MS (SI, **Figure S3**) to confirm end group structure. The ESI-MS shows that a single end group from the initiator ligand remains on each polymer, suggesting linear chain growth proceeding from the $BnSAlMe_2$ initiator.

We investigated the polymerization kinetics of PS in the presence of only initiator ($BnSAlMe_2$), only catalyst (NAI), and both catalyst and initiator. For each experiment, we targeted 20 kg/mol PPS. The polymerization kinetics were determined by monitoring the monomer conversion with ^{1}H NMR spectroscopy over time and a linear fit to $-\ln([PS]/[PS]_0)$ vs. time was used to determine the observed rate constant (k_{obs}). The kinetic plots and SEC traces for each sample can be seen in **Figure 2a** and **Figure 2b**, respectively. For the case with catalyst and initiator, the polymerization proceeded swiftly, and the k_{obs} was found to be (1.67 ± 0.19) $\times 10^{-3}$ s^{-1}, which corresponds to conversion > 95% after time < 1 hour. Furthermore, characterization with SEC reveals a $\overline{M}_n$ = 21.2 kg/mol with a Đ = 1.23, in line with the targeted $\overline{M}_n$. The first order in monomer nature of the kinetics and low Đ suggests the PS polymerization is living. The turnover frequency (TOF) was also calculated and found to be 40.4 hr^{-1}. Unexpectedly, the polymerization rate of PS with only initiator k_{obs} = (1.30 ± 0.16) × 10^{-3} s^{-1} was comparable to PPS synthesized using NAI and $BnSAlMe_2$. However, the $\overline{M}_n$ obtained from SEC for the PPS is 45.3 kg/mol, with Đ = 1.30 more than double the targeted $\overline{M}_n$. In the presence of only NAI, PS polymerizes markedly slower than using both catalyst and the initiator with a k_{obs} of (1.32 ± 0.04) × 10^{-5} s^{-1} which has an $\overline{M}_n$ = 47.6 kg/mol and Đ = 1.31, determined by SEC, which also suggests a lack of control. The fact that the presence of only catalyst is sufficient to polymerize PS is in stark contrast to what is observed with epoxides, in which no polymerization occurs without presence of both catalyst and initiator.[26, 27] We do not think this polymerization is the PPS synthesized with only NAI is a classic Lewis pair polymerization; however, without the initiator the $\overline{M}_n$ cannot be controlled due to irreversible interaction of Lewis pairs (LP) which causes low initiator efficiency and it is the case for several reported LP systems.[34-36] Therefore, catalyst and initiator together are involved in a Lewis pair assisted coordination insertion mechanism with an anionic character for PS polymerization.

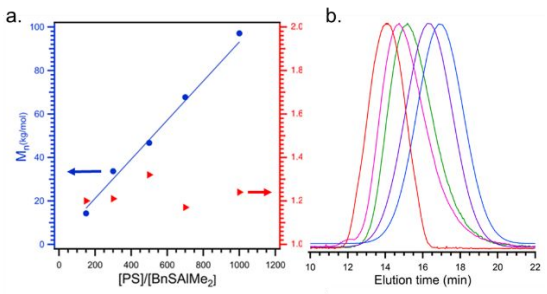

Figure 1. a) Plot of $\overline{M}_n$ (left axis, blue circles) and Đ (right axis, red triangles) as a function of the PS to $BnSAlMe_2$ ratio ($[PS]/[BnSAlMe_2]$). $\overline{M}_n$ increased linearly at increasing ratio of propylene sulphide with Đ < 1.4. b) SEC traces for PPS with different targeted molecular weights, corresponding to entries 1-5 in **Table 1**.

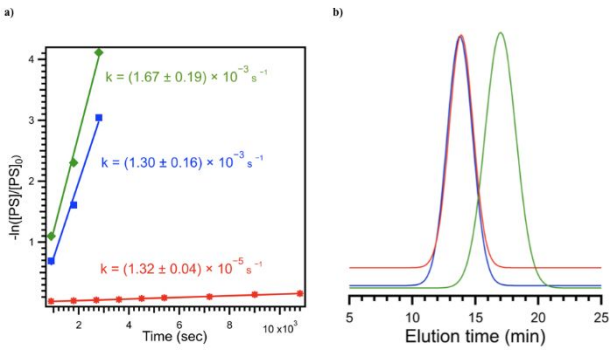

Figure 2. a) Plot of $-\ln([PS]/[PS]_0)$ over time with $BnSAlMe_2$ initiator and NAl catalyst (green line), with only $BnSAlMe_2$ initiator (blue line), and with only NAl catalyst (red line), for polymerization of targeted 20 kg/mol PS. Monomer concentration was monitored via ^{1}H NMR spectroscopy, and the rate of reactions calculated based on it. The rates are as followings from the slope of each plot, k_{obs} = (1.67 ± 0.19) × 10^{-3} s^{-1} with both catalyst and initiator, k_{obs} = 1.32 ± 0.04 × 10^{-5} s^{-1} with only catalyst. b) SEC traces from RI of targeted 20 kg/mol PPS with both the catalyst and the initiator (green), with only the catalyst (red), and with only the initiator (blue). With both the catalyst and the initiator the $\overline{M}_n$ is close to the targeted $\overline{M}_n$, $\overline{M}_n$ = 21.2 kg/mol and Đ of 1.23. However, by using only the catalyst and only the initiator we lose the control over the $\overline{M}_n$. For only catalyst, the $\overline{M}_n$ = 47.6 kg/mol and Đ of 1.31 and only initiator the $\overline{M}_n$ = 45.3 kg/mol with Đ of 1.30.

The relatively high Đ of the PPS coupled with the NAl catalyst only polymerization result was curious. Other synthetic methods for PPS such as, acyl group transfer and AROP, consistently achieve PPS with Đ less than 1.1, but they also typically produce polymers of less than 10 kg/mol.[10, 37] Rumyantsev recently achieved high molecular weight PPS with Đ consistent with our results.[9] However, PS polymerization in the presence of NAl catalyst only without any initiator made us consider other possibilities. To this end, we characterized the as-purchased PS monomer with ^{1}H NMR spectroscopy as well as correlation spectroscopy (COSY). The resulting spectra can be found in SI (**Figures S4**-**S6**). The spectra revealed PS monomer as the majority species, but with small amounts of butane thiol (*ca*. 1.6 mol%) and propene thiol (*ca.* 0.28 mol%). We think this becomes deprotonated in the presence of the NAl catalyst and acts as an initiator for the polymerization of PS, which would be consistent with the slow kinetics. We think this is also partially to blame for our large Đ; over time, during the polymerization, more initiators become active which result in broader molecular weight distribution. This is consistent with our Đ generally increasing with increasing molecular weight and / or polymerization time.

We investigated the statistical copolymerization of PS with epoxides to tune polymer composition. Combining PS with functional epoxides could lead to new biologically relevant materials. Inoue noted the difficulty in typical epoxide-episulphide copolymerization due to the increased reactivity of the episulphide over the epoxide.[38] We copolymerized epichlorohydrin (ECH) and propylene oxide (PO) with PS (**Scheme 2a**) in a 1:1 molar ratio with a targeted molecular weight of 30 kg/mol in the presence of $BnSAlMe_2$ and NAl at 50 °C to achieve statistical copolymers, poly(ECH-*stat*-PS) and poly(PO-*stat*-PS), respectively. The copolymerizations were monitored by ^{1}H NMR spectroscopy, and the reactivity ratios fit to the nonterminal copolymerization model reported by Beckingham–Sanoja–Lynd (BSL)[39] (**Figure 3**). For poly(ECH-*stat*-PS), the reactivity ratios for ECH (r_{ECH}) and PS (r_{PS}) were determined to be r_{ECH} = 0.906 ± .043 and r_{PS} = 1.191 ± 0.059 and for poly(PO-*stat*-PS), the r_{PO} and r_{PS} were calculated to be r_{PO}= 0.905 ± 0.082 and r_{PS} = 1.138 ± 0.108, commensurate with a statistical copolymer that favors PS over epoxide addition. From DSC analysis, P(ECH-*stat*-PS) and P(PO-*stat*-PS) presented only one glass transition temperature (T_g) at –40 °C and –46 °C, respectively, consistent with a statistical copolymer of these two monomers (SI, **Figure S 7**). ^{1}H and ^{13}C NMR spectra were also taken for P(ECH-*stat*-PS) and P(PO-*stat*-PS) (SI, **Figures S8** and **S9**, respectively). The ^{13}C NMR spectra revealed broad peaks associated with PO/ECH and PS as well as mixed heterotriad peaks from adjacent epoxide and episulphide consistent with a statistical copolymer. For instance, for P(ECH-*stat*-PS), a new peak at *ca.* 75 ppm is present which is the methylene adjacent to both an oxygen and a carbon adjacent to a sulphur. This indicates an ECH monomer between two PS monomers. Furthermore, the peak at 45 ppm remains, which belongs to the carbon adjacent to the chlorine atom. This peak would be eliminated if a side reaction through the chloromethyl had occurred. Other crosspeaks are present as well, consistent with the formation of statistical copolymers. SEC and diffusion ordered spectroscopy (DOSY) further corroborate the copolymer structure. SEC (SI, **Figure S 10**) showed a single peak with $\overline{M}_n$ of 29.2 kg/mol and Đ of 1.56 for poly(ECH-*stat*-PS) (**Table 1**, entry 6) and $\overline{M}_n$ of 30.8 kg/mol and Đ of 1.21 for poly(PO-*stat*-PS) (**Table 1**, entry 7). It is unclear why the Đ is much higher for the ECH containing copolymer when compared with the PO containing copolymer. From the ^{1}H and ^{13}C NMR spectra, there are no additional peaks or suppressed peaks due to an unexpected side reaction. To further elaborate on this point, we have previously demonstrated the copolymerization of ECH and other epoxides, like PO.[26] Side reactions that would occur between ECH and PS would also likely to occur between ECH and PO, which were not observed. Furthermore, the DOSY spectra (**Figure 4**, **a** and **b**) exhibit the same diffusion coefficient for all the protons pertaining to the polymers, confirming only one size polymer species is present, which further suggests side reactions are not occurring.

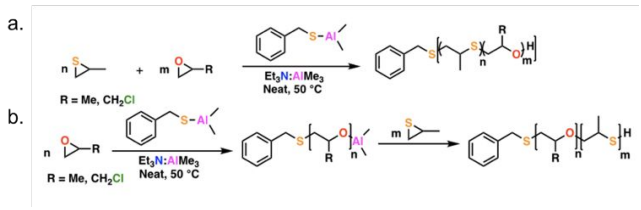

Scheme 2. Statistical (a) and block (b) copolymerization of PS and epoxides.

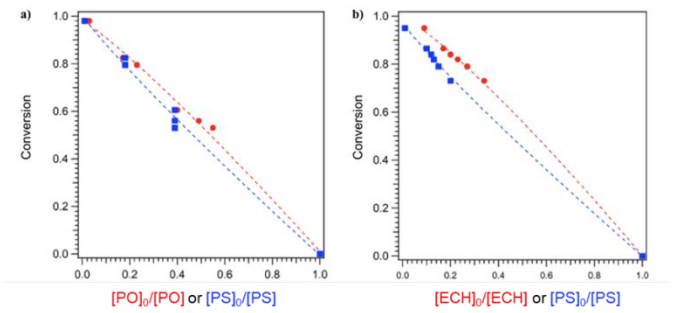

Figure 3. Total conversion as a function of normalized monomer concentration for (a) poly(PO-*stat*-PS) and (b) poly(ECH-*stat*-PS). A fit to this data results in the reactivity ratios for each monomer. The reactivity ratios of the monomer pairs are determined to be r_{PO}= 0.905 ± 0.082 and r_{PS} = 1.138 ± 0.108 for poly(PO-*stat*-PS) and r_{ECH} = 0.906 ± 0.043 and r_{PS} = 1.191 ± 0.059 for poly(ECH-*stat*-PS).

We further synthesized block copolymers of PS and ECH or PO via sequential addition initiated with $BnSAlMe_2$ (**Scheme 2, b**) in the presence of NAl to obtain poly(ECH-*b*-PS) and poly(PO-*b*-PS), respectively. The synthetic method does not require any intermediate steps and epoxide or PS can be directly polymerized from the living chain end of the other. DOSY of the copolymers revealed that the resonances of PECH or PPO and those of PPS corresponded to similar diffusion coefficient for both block copolymers, at 6.37 × 10^{-7} cm^2/sec for P(ECH-*b*-PS) and 1.17 × 10^{-6} cm^2/sec for P(PO-*b*-PS) (**Figure 4**, **c and d).** This finding suggests that both blocks are in the same polymer chain. Both copolymers were characterized by SEC where poly(ECH-*b*-PS) had an $\overline{M}_n$= 29.9 kg/mol and Đ = 1.74 (**Table 1**, entry 8) and poly(PO-*b*-PS) had an $\overline{M}_n$= 29.6 kg/mol and Đ = 1.32 (**Table 1**, entry 9) and (SI, **Figure S 11**). The Đ for the poly(ECH-b-PS) copolymer is high. We think this may be due to the efficiency of the addition of the PS monomer to the living PECH chain end. The results from the statistical copolymerization of ECH and PS reveal a polymer with gradient character, due to the preference of ECH addition over PS. We hypothesize, therefore, that chains that have added PS monomers are favoured for further growth of PS, which results in the high Đ. We have previously characterized homopolymers of PECH and PPO in a previous publication and the Đ for these polymers was significantly more narrow. Furthermore, inspection of the ^{1}H and ^{13}C NMR spectra reveal peaks consistent with a linear block copolymer. Therefore, the efficiency of the PS addition to an epoxide chain end is the most likely culprit. For P(ECH-*b*-PS), two T_g at -29 °C and -40 °C were observed for PECH block and PS block, respectively (SI, **Figure S 12 a**). For P(PO-*b*-PS), we observed two T_g at –70 °C and –47 °C, in agreement with expected values (SI, **Figure S 12 b**). We further characterized the poly(ECH-*b*-PS) and poly(PO-*b*-PS) with ^{1}H and ^{13}C NMR (SI, **Figures S13** and **S14**, respectively). Both sets of NMR spectra are consistent with the formation of block copolymers and no cross peaks are present on the ^{13}C NMR spectrum for either copolymer. Small-angle x-ray scattering (SAXS) revealed a weak shoulder peak at Q ~0.015 $Å^{-1}$, indicating weak phase separation behaviour for Poly(ECH-b-PS) block copolymer (SI, **Figure S 15**) consistent with the DSC results. The Q is the scattering wave-vector. Therefore, this is a facile method to produce functional block copolymers of PS and epoxide.

As mentioned, true statistical copolymers of episulphides and epoxides were difficult to achieve in the past due to episulphide's proclivity to homopolymerize when initiated by the thiolate ion. However, in this work, we were able to achieve statistical copolymers of these two disparate monomers suggesting that PS can add similarly as well to what we

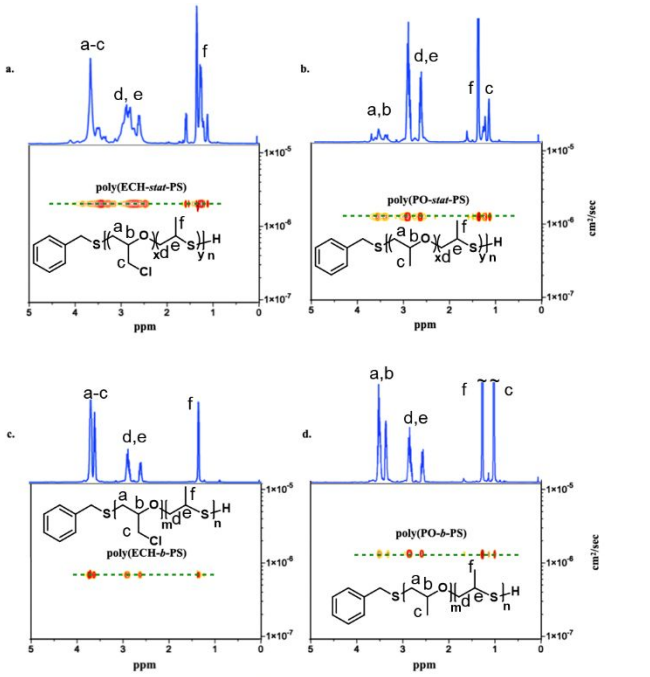

Figure 4. DOSY NMR of statistical copolymers (a and b) and block copolymers (c and d). The DOSY spectra reveal that there is only one diffusing species for both the statistical and block copolymers, indicating that both monomers share a common backbone.

hypothesize to be a thiolate (from the PS) or oxyanion (from the epoxide) polymer chain end. We, therefore, wondered: does the initiating anion matter? To this end, we polymerized PS from a benzyl alcohol aluminium initiator ($BnOAlMe_2$) in the presence of NAl catalyst, as shown in **Scheme 3**. The resultant PPS was characterized by ^{1}H and ^{13}C NMR spectroscopy (SI, **Figure S 16)** and $\overline{M}_n$ (SI, **Figure S 17**), characterized by SEC. Both the ^{1}H and ^{13}C NMR spectra were similar to the PPS initiated by the SAI. The $\overline{M}_n$ was found to be 31.7 kg/mol from SEC which compared favourably with the targeted $\overline{M}_n$ of 30 kg/mol with Đ =1.24. The T_g was also determined for this polymer from DSC and found to be –42 ºC (SI, **Figure S 18**), consistent with the PPS initiated from $BnSAlMe_2$. The difference between the PPS initiated by $BnOAlMe_2$ and $BnSAlMe_2$ was the overall polymerization time. PS was > 99% converted after 48 hours with $BnOAlMe_2$ compared with 10 hours for $BnSAlMe_2$. It has been previously noted[40] that the electronegativity of the substituent groups at the aluminium can have a significant effect on the propagation rate for polymerization of heterocycles (*i.e.*, lactones) and so the difference may be due to the difference in electronegativity between sulphur and oxygen. Ultimately, this result suggests that a PS polymerization initiated by either the oxyanion or the thiolate proceed by the

same mechanism, but with the oxyanion initiated polymerization proceeding more slowly. This may explain why we are able to achieve statistical copolymers of epoxides and PS. Work is ongoing to better understand this interaction.

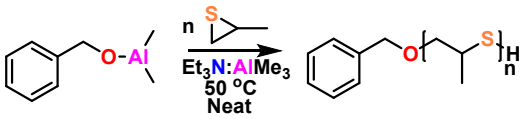

Scheme 3. $BnOAlMe_2$ initiated PS polymerization

Inspired by the previous reports of PS containing ABA polymers,[10, 11] we investigated (co)polymer architecture through initiator design. Specifically, a di-functional (d-H) (**Figure 5**, compound 1) initiator was synthesized from 1,3 propane dithiol with trimethylaluminium at –78 °C. The d-H initiator was characterized by ^{1}H and ^{13}C NMR spectroscopy as well as ^{1}H – ^{1}H correlated spectroscopy (COSY). The NMR spectra of the d-H initiator were consistent with our suggested structure. (SI, **Figures S19** and **S20**).

The d-H initiator was used to synthesize linear PPS (**Figure 5 a**, compound 2). The homopolymer was characterized by SEC (SI, **Figure S 21**) with $\overline{M}_n$ = 34.5 and Đ = 1.37 (**Table 1**, Entry 10), consistent with the targeted molecular weight of 30 kg/mol. To test whether the PPS formed from both ends of the d-H initiator, we conducted a kinetic study. The d-H initiator and an analogous mono-functional initiator ($PrSAlMe_2$) polymerized PS at a controlled monomer to initiator ratio at 50 °C. The reactions were monitored over time by ^{1}H NMR spectroscopy, and the -ln([PS]/[PS]$_0$) vs. time (s) was plotted to determine k_{obs}, as seen in **Figure 6**. From the slope of the fit, the rate constant was calculated to be k_{obs} = (7.11 ± 0.59) × 10^{-5} s $^{-1}$ ($PrSAlMe_2$) and (15.9 ± 0.86) × 10^{-5} s $^{-1}$ (d-H). The polymerization is approximately twice as fast for the d-H initiator than for the mono-functional initiator, commensurate with propagation co-occurring at two ends.

The d-H initiator was used to synthesize an ABA tri-block-copolymer (**Figure 5**, compound 3) of PS and PO through sequential addition. The resultant copolymer was characterized by ^{1}H and ^{13}C NMR spectroscopy and the spectroscopic peaks were commensurate with the anticipated polymer structure (SI, **Figure S 22**). A DOSY experiment, **Figure 7**, revealed a single diffusion coefficient for all polymer peaks. The copolymer was further characterized by SEC (SI, **Figure S 23**) (**Table 1**, entry 11) with the $\overline{M}_n$ = 29.8 kg/mol and Đ = 1.39, which is consistent with the targeted $\overline{M}_n$ of 30 kg/mol.

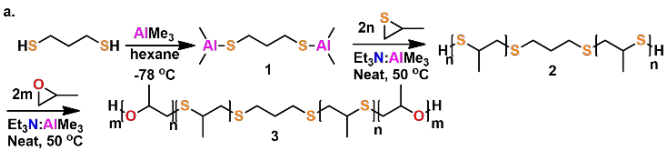

Figure 5. Chemical reaction scheme for the synthesis of d-H initiator followed by PPS synthesis from d-H initiator and copolymerization.

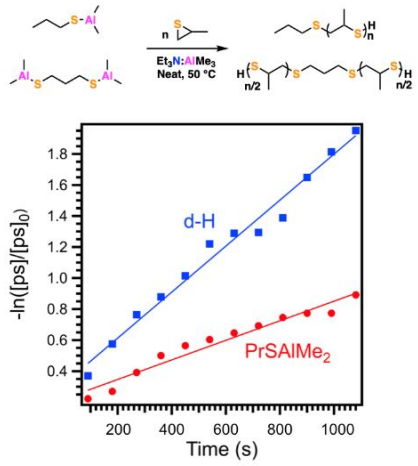

Figure 6. (top) Reaction scheme for the d-h or $PrSAlMe_2$ initiated polymerization of PS. (bottom) Plot of normalized PS concentration over time with $PrSAlMe_2$ initiator and NAl catalyst (red line) and with d-H initiator and NAl catalyst (blue line). From the slope of the fit, the rate constant was calculated to be k_{obs} = (7.11 ± 0.59) × 10^{-5} s $^{-1}$ ($PrSAlMe_2$) and (15.9 ± 0.86) × 10^{-5} s $^{-1}$ (d-H). The rate of polymerization is as twice as fast for d-H initiator in comparison with $PrSAlMe_2$, suggesting that the initiation is happening from both ends of the initiator.

DSC (SI, **Figure S 24**) of the copolymer revealed two T_g at –66 °C and –45 °C, which agrees with the block-copolymer architecture. Furthermore, SAXS reveals clear micro-phase separation for the triblock copolymer synthesized with a notable peak at Q ~ 0.02 $Å^{-1}$. (SI, **Figure S 25**). Therefore, this polymerization method allows us to synthesize block copolymers of PS and epoxide and allows us to tune polymer architecture through initiator design.

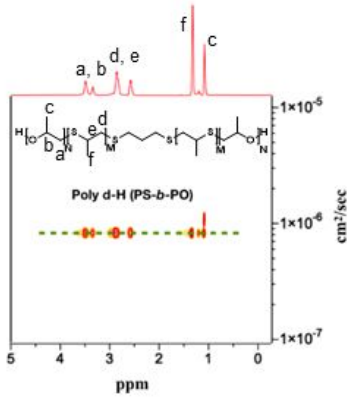

Figure 7. DOSY NMR of poly d-H (PS-b-PO). The results suggest both the epoxide and PS are in the same polymer chain.

Finally, we synthesized a block copolymer consisting of ethylene glycol (EG) and PS units to further demonstrate the utility of our synthetic platform. PEG-b-PS is an important polymer in drug delivery applications and is often synthesized through a multi-step process. Here, we reacted 5 kg/mol monomethyl ether-PEG (mPEG) with $AlMe_3$ in benzene to create a macroinitiator $mPEGAlMe_2$, as seen in **Figure 8** a. PS was then polymerized from the end of the $mPEGAlMe_2$ in benzene at 50 ºC in the presence of NAl catalyst. The final PEG-*b*-PPS was characterized

via ^{1}H NMR and ^{13}C NMR spectroscopy (SI, **Figure S 26**) as well as DOSY NMR, **Figure 8** b. The ^{1}H and ^{13}C NMR spectra were consistent with the anticipated block-co-polymer and the DOSY NMR revealed a single diffusion coefficient, suggesting PEG and PPS units are in the same polymer chain. The mPEG and PEG-*b*-PPS was also characterized via SEC and the LS traces can be seen in **Figure 8 c**. A shift to a lower retention time can be seen upon polymerization of PPS from the mPEGAlMe$_2$ macroinitiator, consistent with the expected increase in the molecular weight. The SEC of mPEG revealed a $\overline{M}_n$ of 5.5 kg/mol and Đ of 1.24, matching data provided by the vendor. The SEC of the block-co-polymer revealed a $\overline{M}_n$ of 22.2 kg/mol and Đ = 1.18, commensurate with the targeted $\overline{M}_n$. Finally, DSC (SI, **Figure S 25**) revealed a single T_g at –41 ºC, matching that of the PPS block, and a melting point (T_m) of 58 ºC, consistent with the thermal data provided by the vendor. The T_g of the PEG block is not evident as it is most likely out of the temperature range accessible by our DSC, but the appearance of the T_m is strong evidence the PEG block is present. Therefore, we have demonstrated a facile method to produce PEG-*b*-PPS *via* our method.

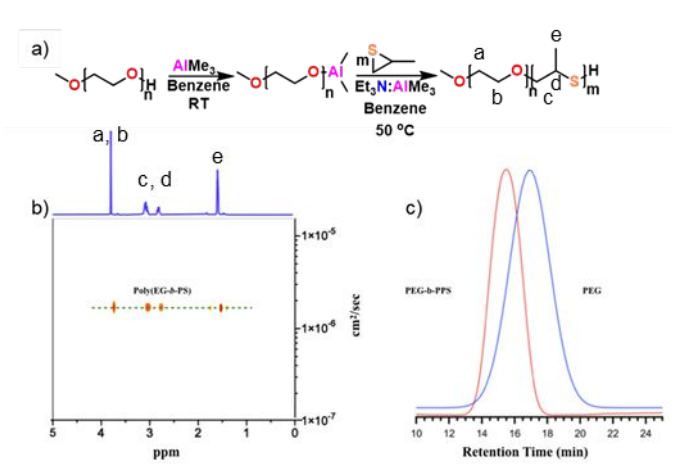

Figure 8. a) Scheme for synthesis of PEG-*b*-PPS. b) DOSY NMR PEG-*b*-PPS c) SEC traces (LS) of PEG (right, blue curve) and PEG-*b*-PPS (left, red curve). The $\overline{M}_n$ and Đ were determined to be, respectively, 5.5 kg/mol and 1.24 (PEG) and 22.2 kg/mol and 1.18 PEG-*b*-PPS

Conclusions

In summary, we presented a new methodology for (co)polymerization of PS with a recently reported SAl initiator. This method is living and produces polymers with controlled molecular weight up to 100 kg/mol and low Đ. We demonstrated statistical copolymerization of PS and epoxides to obtain unique, compositionally controlled copolymers. Polymer structure was characterized by various means such as ^{1}H and ^{13}C NMR spectroscopy, DOSY, SEC, DSC, and SAXS. Further, the chemical flexibility of our SAl initiators enabled us to impart architectural control on the PS containing (co)polymers in the form of an ABA copolymer. Finally, we synthesized a PEG-b-PPS from a PEG macroinitiator and characterized it by ^{1}H and ^{13}C NMR spectroscopy, DOSY, DSC, and SEC. This facile and tuneable aluminium initiator system opens the door for a more robust and controlled synthesis of PS-epoxide copolymers that can be applied in biomedical and other contexts.

Author Contributions

The manuscript was written through contributions of all authors. All authors have given approval to the final version of the manuscript.

Conflicts of interest

There are no conflicts to declare.

Acknowledgements

The authors acknowledge the partial support of this work through the Collaborative Research Program of the Institute for Chemical Research, Kyoto University (Grant nos. 2020-75, 2021-76). R.C.F. acknowledges the start-up support from the Department of Chemical Engineering and Materials Science at MSU. K.O. acknowledges the funding from the Japan Society for the Promotion of Science (JSPS) KAKENHI Grants (no. 18H02033). S.C. acknowledges the financial support from the College of Engineering at MSU. The SAXS measurements were performed at Beamline 12-ID-B of Advanced Photon Source, a U.S. Department of Energy (DOE) Office of Science User Facility operated for the DOE Office of Science by Argonne National Laboratory under Contract No. DE-AC02-06CH11357.

References

1. C. A. Ford, T. J. Spoonmore, M. K. Gupta, C. L. Duvall, S. A. Guelcher and J. E. Cassat, *Journal of Orthopaedic Research*, 2021, **39**, 426-437.
2. S. T. Reddy, A. Rehor, H. G. Schmoekel, J. A. Hubbell and M. A. Swartz, *J. Controlled Release*, 2006, **112**, 26-34.
3. S. Hirosue, I. C. Kourtis, A. J. van der Vlies, J. A. Hubbell and M. A. Swartz, *Vaccine*, 2010, **28**, 7897-7906.
4. J. P. Bearinger, G. Stone, A. L. Hiddessen, L. C. Dugan, L. Wu, P. Hailey, J. W. Conway, T. Kuenzler, L. Feller, S. Cerritelli and J. A. Hubbell, *Langmuir : the ACS journal of surfaces and colloids*, 2009, **25**, 1238-1244.
5. L. Feller, J. P. Bearinger, L. Wu, J. A. Hubbell, M. Textor and S. Tosatti, *Surf. Sci.*, 2008, **602**, 2305-2310.
6. C. D. Vo, G. Kilcher and N. Tirelli, *Macromol. Rapid Commun.*, 2009, **30**, 299-315.
7. F. Du, B. Qiao, T. D. Nguyen, M. P. Vincent, S. Bobbala, S. Yi, C. Lescott, V. P. Dravid, M. Olvera de la Cruz and E. A. Scott, *Nature Communications*, 2020, **11**, 4896.
8. S. Boileau, G. Champetier and P. Sigwalt, *Makromolekulare Chemie*, 1963, **69**, 180-192.
9. M. Rumyantsev, *Polymer Chemistry*, 2021, **12**, 1298-1309.
10. A. Rehor, N. Tirelli and J. A. Hubbell, *Macromolecules*, 2002, **35**, 8688-8693.
11. A. J. van der Vlies, C. P. O'Neil, U. Hasegawa, N. Hammond and J. A. Hubbell, *Bioconjugate Chem.*, 2010, **21**, 653-662.

12. A. Suzuki, D. Nagai, B. Ochiai and T. Endo, *Macromolecules*, 2004, **37**, 8823-8824.
13. A. Napoli, M. Valentini, N. Tirelli, M. Müller and J. A. Hubbell, *Nature Materials*, 2004, **3**, 183-189.
14. A. E. Vasdekis, E. A. Scott, C. P. O'Neil, D. Psaltis and J. A. Hubbell, *ACS Nano*, 2012, **6**, 7850-7857.
15. Y. Lee, H. Koo, G.-w. Jin, H. Mo, M. Y. Cho, J.-Y. Park, J. S. Choi and J. S. Park, *Biomacromolecules*, 2005, **6**, 24-26.
16. A. Napoli, N. Tirelli, G. Kilcher and A. Hubbell, *Macromolecules*, 2001, **34**, 8913-8917.
17. M. Frey, M. Vincent, S. Bobbala, R. Burt and E. Scott, *Chem. Commun.*, 2020, **56**, 6644-6647.
18. C.-H. Wang, Y.-S. Fan, Z. Zhang, Q.-B. Chen, T.-Y. Zeng, Q.-Y. Meng and Y.-Z. You, *Appl. Surf. Sci.*, 2019, **475**, 639-644.
19. Y. Tang, C. Pina-Hernandez, Q. Niu, J. Nie and S. Cabrini, *Journal of Materials Chemistry C*, 2018, **6**, 8823-8831.
20. J. P. Bell, T.-M. Don, S. Voong, A. Fernandez and W. Ku, *Die Angewandte Makromolekulare Chemie*, 1996, **240**, 67-81.
21. C.-J. Zhang, T.-C. Zhu, X.-H. Cao, X. Hong and X.-H. Zhang, *Journal of the American Chemical Society*, 2019, **141**, 5490-5496.
22. K. Nakano, G. Tatsumi and K. Nozaki, *Journal of the American Chemical Society*, 2007, **129**, 15116-15117.
23. C. C. J. Culvenor, W. Davies and N. S. Heath, *Journal of the Chemical Society (Resumed)*, 1949, DOI: 10.1039/JR9490000282, 282-287.
24. *USA Pat.,* 3000865, 1958.
25. *USA Pat.,* 2484370, 1946.
26. N. Safaie, B. Rawal, K. Ohno and R. C. Ferrier, *Macromolecules*, 2020, **53**, 8181-8191.
27. J. Imbrogno, R. C. Ferrier, B. K. Wheatle, M. J. Rose and N. A. Lynd, *ACS Catalysis*, 2018, **8**, 8796-8803.
28. N. Safaie, B. Rawal, K. Ohno and R. C. Ferrier, *Macromolecules*, 2020, DOI: 10.1021/acs.macromol.0c00464.
29. C. Billouard, S. Carlotti, P. Desbois and A. Deffieux, *Macromolecules*, 2004, **37**, 4038-4043.
30. A. Labbé, S. Carlotti, C. Billouard, P. Desbois and A. Deffieux, *Macromolecules*, 2007, **40**, 7842-7847.
31. S. Carlotti, A. Labbé, V. Rejsek, S. Doutaz, M. Gervais and A. Deffieux, *Macromolecules*, 2008, **41**, 7058-7062.
32. J. Imbrogno, DOI: 10.26153/tsw/13867, University of Texas at Austin, 2021.
33. E. Nicol, T. Nicolai and D. Durand, *Macromolecules*, 1999, **32**, 7530-7536.
34. Y. Zhang, G. M. Miyake and E. Y.-X. Chen, *Angew. Chem. Int. Ed.*, 2010, **49**, 10158-10162.
35. Y. Zhang, G. M. Miyake, M. G. John, L. Falivene, L. Caporaso, L. Cavallo and E. Y. X. Chen, *Dalton Transactions*, 2012, **41**, 9119-9134.
36. E. Y.-X. Chen, in *Frustrated Lewis Pairs II: Expanding the Scope*, eds. G. Erker and D. W. Stephan, Springer Berlin Heidelberg, Berlin, Heidelberg, 2013, DOI: 10.1007/128_2012_372, pp. 239-260.
37. A. Nagai, N. Koike, H. Kudo and T. Nishikubo, *Macromolecules*, 2007, **40**, 8129-8131.
38. Y. Watanabe, T. Aida and S. Inoue, *Macromolecules*, 1991, **24**, 3970-3972.
39. N. A. Lynd, R. C. Ferrier and B. S. Beckingham, *Macromolecules*, 2019, **52**, 2277-2285.
40. A. Duda and S. Penczek, *Makromolekulare Chemie. Macromolecular Symposia*, 1991, **47**, 127-140.